Journal of ELECTRONIC MATERIALS, Vol. 39, No. 9, 2010
DOI: 10.1007/s11664-010-1277-2

Characteristics of a Pin–Fin Structure Thermoelectric Uni-Leg Device Using a Commercial *n*-Type Mg_2Si Source

TAKASHI NEMOTO,[1,3] TSUTOMU IIDA,[2] JUNICHI SATO,[1] YOHEI OGUNI,[2] ATSUNOBU MATSUMOTO,[2] TAKAHIRO MIYATA,[2] TATSUYA SAKAMOTO,[2] TADAO NAKAJIMA,[1] HIROHISA TAGUCHI,[2] KEISHI NISHIO,[2] and YOSHIFUMI TAKANASHI[2]

1.—Nippon Thermostat Co., Ltd., 6-59-2 Nakazato, Kiyose-shi, Tokyo 204-0003, Japan. 2.—Department of Materials Science and Technology, Tokyo University of Science, 2641 Yamazaki, Noda-shi, Chiba 278-8510, Japan. 3.—e-mail: tnemoto@ntcl.co.jp

Mg_2Si thermoelectric (TE) elements and modules were fabricated using a commercial polycrystalline Mg_2Si source. A monobloc plasma-activated sintering technique was used to fabricate the TE elements and Ni electrodes. The TE modules were composed of *n*-type Mg_2Si, using pin–fin structure elements, in order to achieve simple assembly and to realize stable operation at a temperature of ~800 K. The dimensions of each pin–fin element were 4.2 mm × 4.2 mm × 9.8 mm, and the TE module comprised nine pin–fin elements connected in series. The output characteristics of the pin–fin elements and the TE module were evaluated at temperature differences, ΔT, ranging from 100 K to 500 K. The observed values of open-circuit voltage (V_{OC}) and output power (P) of a single pin–fin element were 98.7 mV and 50.9 mW, respectively, at the maximum ΔT of 500 K. The maximum V_{OC} and P values for the TE module were 588 mV and 174.3 mW, respectively, at ΔT = 500 K.

Key words: Mg_2Si, thermoelectric module, uni-leg, plasma-activated sintering, silicide, output power

INTRODUCTION

The relentless increase in the concentration of atmospheric CO_2 due to the increase in energy generation using fossil fuels is accelerating global warming.[1] In attempts to alleviate this problem, solar and wind power have already been turned to practical use. However, integration of these new energy generation systems has been slow and protracted. Thus, improving the potential conversion efficiency of conventional power generation is still an important issue. Thermoelectric (TE) power generation, i.e., direct energy conversion from heat to electrical power, can contribute to improving the potential conversion efficiency of existing power generators.[2] So far, there are only a few commercially available TE generators, such as, for example, the Bi-Te system. However the Bi-Te TE module is unsuitable for use at temperatures much above 400 K,[3] and its constituent elements are toxic. On the other hand, magnesium silicide (Mg_2Si) has been identified as a promising advanced TE material, operating at temperatures ranging from 500 K to 800 K. Its properties, such as being an environmentally benign material, the abundance of its constituent elements in the Earth's crust, and the nontoxicity of its processing by-products, make Mg_2Si an attractive material for TE generation.[4–7] Moreover, the dimensionless figure of merit, ZT, characterizing the efficiency of a TE material, for *n*-type Mg_2Si has already reached ~1.0 at 873 K.[8] Although a large number of studies have been done on the TE characteristics of Mg_2Si,[9–14] the output characteristics of Mg_2Si TE elements and modules have not been sufficiently investigated.

(Received July 10, 2009; accepted May 7, 2010; published online June 3, 2010)

When TE power generation is applied to large-scale systems, both the output voltage and the output current of the modules need to be configured by combining the elements in the modules in both series and parallel connections. Connecting elements in parallel offers a fail-safe composition for the module, because, even if one element is damaged, the output from the module might not be completely lost. In this study, a pin–fin structure TE element was developed as a means of electrically connecting elements in parallel. For the formation of a module with uni-leg structure, this structure offers simple assembly and suppresses the increase in the connecting regions, resulting in a decrease in the internal resistance of the module, because this element comprises a structure where one side of several pins is connected internally. Additionally, this structure has a fail-safe composition. Even if one pin of the element cracks, the crack cannot spread to the other pins, because each pin is separated by slits.

Additionally, we have fabricated a uni-leg TE module, composed only of n-type Mg_2Si, using nine pin–fin structure TE elements. Compared with the conventional π-structure TE module, which comprises both p- and n-type TE elements, the uni-leg structure reduces the problems associated with thermal expansion differences between p- and n-type TE elements at high temperature.[15]

EXPERIMENTAL PROCEDURES

The starting material for the fabrication of the Mg_2Si TE devices was presynthesized polycrystalline undoped Mg_2Si provided by Union Materials Inc. This presynthesized Mg_2Si was prepared from a mixture containing granular Mg (99.95%) and powdered Si (99.99999%) in stoichiometric ratio of 2:1 and was synthesized in an electric furnace. The polycrystalline Mg_2Si was ground into powder with a particle size of 75 μm or less. The powder was then placed into a graphite die and sintered using an ELENIX plasma-activated sintering (PAS) III-Es. At the same time, Ni electrodes were formed on the Mg_2Si by employing a monobloc PAS technique, performed at 1073 K for 2 min at a pressure of 29.4 MPa in Ar (0.06 MPa) atmosphere. Prior to this research, as reported by Oguni et al.,[16] attempts were made to deposit Cu, Ti, and Ni electrodes on Mg_2Si by employing the same process used in this experiment. However, it appeared that Cu and Ti were unstable in the monobloc sintering process. Therefore, we used Ni for the electrode material in this work. The dimensions of the sintered billet were 15 mm in diameter and 10 mm thick. Pin–fin structure elements were cut from the sintered billet using a wire saw. The shape of a pin–fin element is shown in Fig. 1. The elements had a 4.2 mm × 4.2 mm × 3.0 mm Mg_2Si base, over which four Mg_2Si pins, 6.8 mm tall with a square cross-section of 2 mm × 2 mm, were arranged in a regular pattern. The width of the grooves between each pin was 0.2 mm. The TE module, composed of only n-type Mg_2Si, was fabricated using nine pin–fin structure TE elements, each of which was connected electrically in series using Ni terminals. The Ni terminals connect the hot side of one element with the cold side of its neighboring element. The elements and Ni terminals were joined using silver paste. The fabricated TE module is shown in Fig. 2.

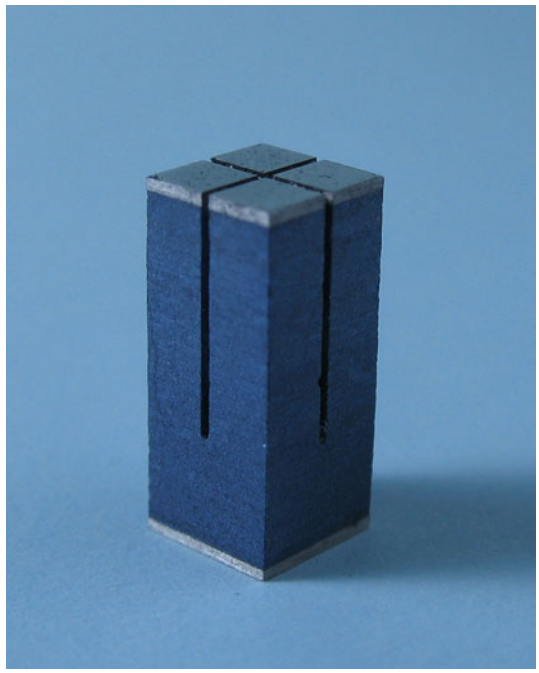

Fig. 1. Pin–fin structure TE element.

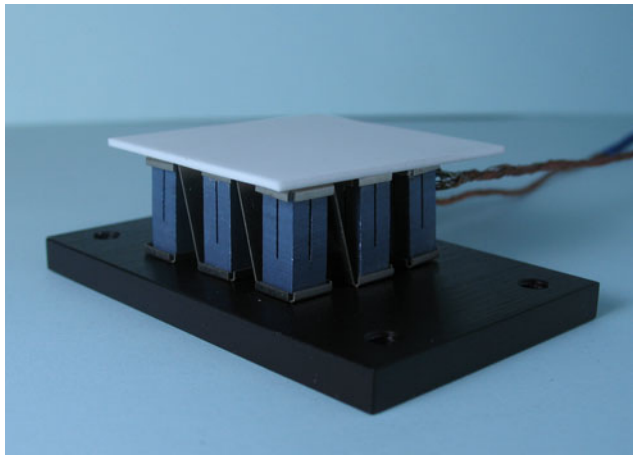

Fig. 2. Uni-leg TE module, consisting of nine pin–fin structure TE elements.

The open-circuit voltage and TE power output with the temperature difference, ΔT, ranging from 100 K to 500 K, were measured in air using a Union Material UMTE-1000M. The top of the element or module was heated by an electrically heated

stainless-steel block, whereas the base was cooled with an aluminum block. Heat to the heating block was provided by an electrical heater at 473 K to 873 K, whereas the cooling block was maintained at 373 K by a combination of water cooling and electrical heating. The output current and output power were measured under closed-circuit conditions, varying the value of the external load. The internal resistance at room temperature of the elements and the module were measured using an ADEX AX-222. The Seebeck coefficient (S) and the electrical resistivity (ρ) of the sintered samples were measured over the temperature range from 350 K to 860 K using ULVAC-RIKO ZEM-2 equipment. The thermal conductivity (κ) was measured over the temperature range from 300 K to 873 K, employing a laser flash method, using a ULVAC-RIKO TC-7000H.

RESULTS AND DISCUSSION

The temperature-dependent S values, ρ values, κ values, and the dimensionless figure of merit, ZT, of sintered undoped Mg_2Si are listed in Table I. $ZT = S^2T/\rho\kappa$, is an index of TE performance and is closely associated with the thermoelectric conversion efficiency. The observed S values were negative in the measured temperature range, indicating n-type conductivity. The absolute value of S increased from 136 μV/K at 373 K to 275 μV/K at 673 K and then decreased to 234 μV/K at 873 K. On the other hand, the ρ value increased from 7.81×10^{-6} Ω m at 373 K to 3.30×10^{-5} Ω m at 673 K and then decreased to 2.09×10^{-5} Ω m at 873 K. The thermal conductivity decreased with increasing temperature. The maximum ZT value was 0.62 at 873 K.

The fabricated elements are listed in Table II, with the dimension or shape of the element, its measured internal resistance, and its manufacturing factor (MF). Samples E-a and E-b were 2 mm $\times$ 2 mm $\times$ 10 mm and 4.2 mm $\times$ 4.2 mm $\times$ 10 mm, respectively. These simply shaped elements were fabricated for comparison with the pin–fin structure element. For the pin–fin structure element, two samples, PFE-a and PFE-b, with different internal resistances were evaluated, because the elements used for the TE module had various internal resistances. These variations were induced during the sintering process. Although all the samples were sintered using the same sequence of controlled temperature, a slight difference in the thickness of the sintered billet was observed. It was found that this slight difference in thickness caused a difference in density giving rise to a variation in internal resistance. More accurate control of the sintering process should solve this problem. The MF, defined as $MF = R_{ideal}/R_{int}$, where R_{ideal} is the theoretical resistance of the element and R_{int} is the actual internal resistance, was introduced in order to interpret the quality of our elements. As shown in Table II, the MF reaches only $\sim$25% for samples E-a, E-b, and PFE-a, and 14% for sample PFE-b. In actual devices there is a contact resistance $R_{contact}$ between the TE material and the metal; thus, the internal resistance R_{int} is given by $R_{int} = R_{ideal} + R_{contact}$. Although the value of MF for sample PFE-b (14%) was lower than that of the other samples, there was no remarkable difference between samples E-a (26%), E-b (23%), and PFE-a (24%). It appears that the value of MF for the pin–fin structure element is little affected by the slit. However, it is important that the value of MF be improved in order to further improve the performance of the element. It is well known that one such improvement can be achieved by using material

Table I. TE properties of source material

Temperature (K)	Seebeck Coefficient (μV/K)	Electrical Resistivity (Ω m)	Thermal Conductivity (W/mK)	Dimensionless Figure of Merit
373	−136	7.81×10^{-6}	7.13	0.12
473	−167	1.29×10^{-5}	5.51	0.19
573	−247	2.83×10^{-5}	4.45	0.28
673	−275	3.30×10^{-5}	4.10	0.38
773	−252	2.51×10^{-5}	3.98	0.49
873	−234	2.09×10^{-5}	3.67	0.62

Table II. List of measured elements

Sample Name	Dimension/ Shape	Measured Internal Resistance of Elements at RT (mΩ)	MF at RT
E-a	2 mm $\times$ 2 mm $\times$ 9.8 mm	76	0.26
E-b	4.2 mm $\times$ 4.2 mm $\times$ 9.8 mm	20	0.23
PFE-a	Pin–fin element	20	0.24
PFE-b	Pin–fin element	34	0.14

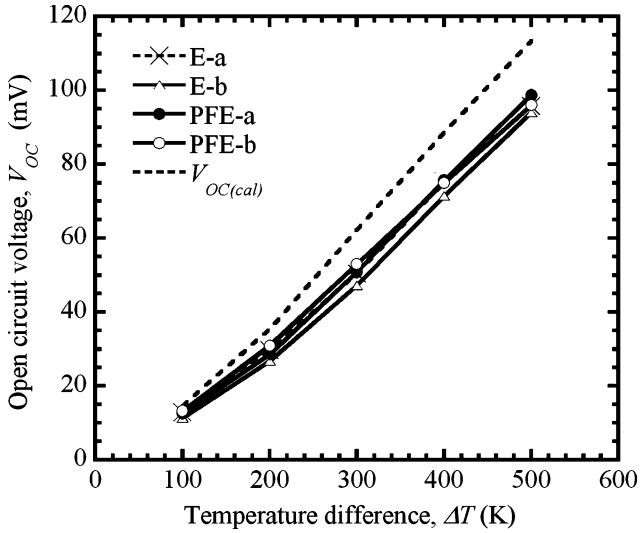

Fig. 3. Measured and calculated open-circuit voltage of the Mg_2Si elements as a function of temperature difference, ΔT, ranging from 100 K to 500 K.

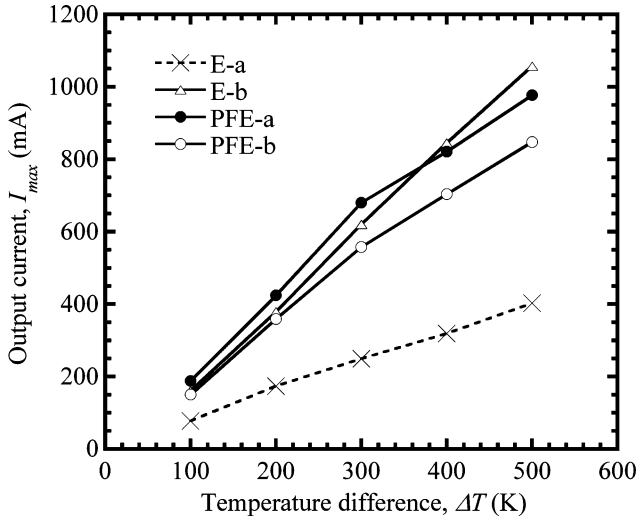

Fig. 4. Measured output current of the Mg_2Si elements as a function of temperature difference, ΔT, ranging from 100 K to 500 K.

more suitable to Mg_2Si for the electrodes. This needs to be studied in a more systematic manner using materials such as transition-metal silicides or Ni-Cu alloy.

The measured open-circuit voltage, V_{OC}, of each sample with respect to temperature difference, ΔT, ranging from 100 K to 500 K, is shown in Fig. 3, together with the calculated value [$V_{OC(cal)}$]. The $V_{OC(cal)}$ value is given by:

$$V_{OC(cal)} = \int_{T_c}^{T_h} S(T)\mathrm{d}T,$$

where T_h is the hot-side temperature, T_c is the cold-side temperature, and S is the measured Seebeck coefficient. The highest measured V_{OC} values for samples E-a, E-b, PFE-a, and PFE-b were 95.8 mV, 94.0 mV, 98.7 mV, and 96.0 mV, respectively, at ΔT = 500 K. When compared with the calculated value, the measured V_{OC} values of all samples were lower. When the temperature difference between the heating and cooling blocks was 500 K, it was estimated that there was a thermal loss of about 50 K between the heating block and the element. Taking this thermal loss into consideration, the measured V_{OC} values are in fair agreement with the calculated one. The observed V_{OC} of the pin–fin structure elements, samples PFE-a and PFE-b, at ΔT = 500 K were slightly larger than that of the simple element, sample E-b, at ΔT = 500 K. The main reason may be that, for the pin–fin elements, the cross-sectional area of the cold sides is larger than those of the hot sides due to the slits. This may give rise to a large temperature difference between the hot and cold sides of the pin–fin element. However, optimization of the dimensions, such as the width and depth of the grooves, the length and thickness of the legs, and the dimensions of the base, may improve the performance of the pin–fin structure element. Also, using a thermal insulator to prevent thermal radiation from the heat source to the slits between each pin may be needed to improve the performance of the pin–fin element.

The measured maximum output current (I_{max}) and maximum output power (P_{max}) with a load resistance for temperature differences, ΔT, ranging from 100 K to 500 K are shown in Figs. 4 and 5, respectively. The I_{max} and P_{max} values of the samples were estimated from the relationships $I_{max} = S(T_h - T_c)/2r$ and $P_{max} = I_{max}^2 r = I_{max}V$, respectively, where P_{max} is the maximum output power under the condition in which the external resistance is the same as the resistance of the element, r, and T_h and T_c are the hot- and cold-side temperatures, respectively. I_{max} and V are the output current and output voltage, respectively, when the output power is at its maximum. The measurements of I_{max} and P_{max} were performed with the load resistance, including the wiring resistance, matched to the internal resistance of each element. Comparing sample E-b with sample PFE-a, which have almost identical size and internal resistance, the measured I_{max} value of sample PFE-a is greater below ΔT = 300 K. On the other hand, above ΔT = 300 K, it is smaller. This is due to the fact that the slope of the measured I_{max} for PFE-a (and PFE-b) changes at ΔT = 300 K; however, the reason for this is still unclear. For sample PFE-b, the measured I_{max} value is lower than that of sample PFE-a. This may be due to high internal resistance in sample PFE-b. Although the values of MF and V_{OC} for samples E-a, E-b, and PFE-a are almost identical, the output current per unit area of sample E-a is larger than those of the others. However, it must be noted that, if sample E-a were to be used for the module, the assembly would be more complex and there might also be a loss of current due to increased

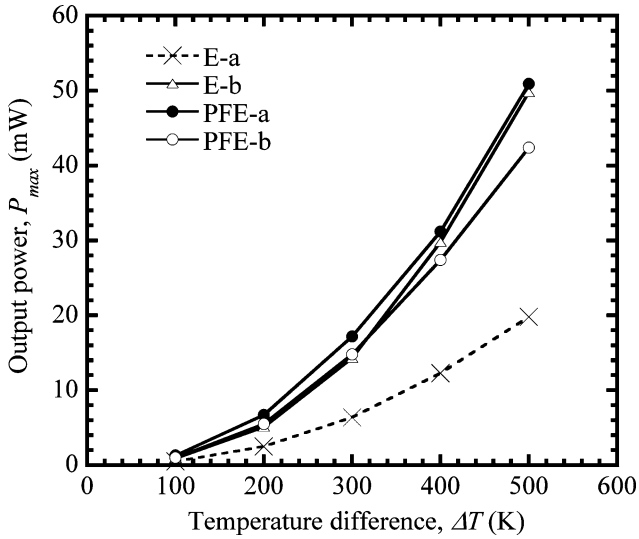

Fig. 5. Measured output power of the Mg_2Si elements as a function of temperature difference, ΔT, ranging from 100 K to 500 K.

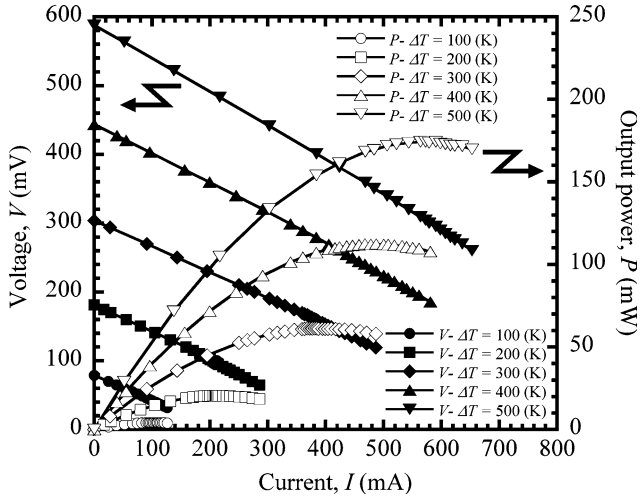

Fig. 6. Output characteristics of the pin–fin structure module for various temperature differences, ΔT.

contact and terminal resistances. On the other hand, although the pin–fin structure element has slits, there is no remarkable difference in the values of I_{max} and V_{OC} between samples PFE-a and E-b. Therefore, there is an advantage in using the pin–fin structure element for the module.

As shown in Fig. 5, the maximum output power, P_{max}, of the elements are 19.8 mW for sample E-a, 49.8 mW for sample E-b, 50.9 mW for sample PFE-a, and 42.4 mW for sample PFE-b, all at ΔT = 500 K. Although the highest output power per unit area was observed for sample E-a, the TE module discussed below was fabricated using the pin–fin structure element. Using this has the advantages of simpler assembly and lower electrical resistance than would be the case with sample E-a, and also has the advantage of a fail-safe composition when compared with sample E-b.

A TE module composed of *n*-type Mg_2Si was fabricated using pin–fin structure TE elements with individual elements connected electrically in series using Ni terminals. Table III shows the number of elements, the total resistance of the elements, and the internal resistance of the module. The total resistance of the elements in the module is 275 mΩ, with the average internal resistance of the elements being 30.6 mΩ. The internal resistance of the module is 320 mΩ. Since the resistance of the Ni terminals used to connect each element together is about 9 mΩ, about 36 mΩ is due to the contact resistance between the elements and the Ni terminals. This terminal and contact resistance has a deleterious effect on the module performance. Thus, it is necessary to improve the means by which the elements are connected if the value of MF is to be improved.

Figure 6 shows the *I*–*V* characteristic and output power of the module for various temperature differences, ΔT, ranging from 100 K to 500 K. The *I*–*V* characteristic of the module is linear over the measured temperature range. The V_{OC} values increase with increasing ΔT, and reach 588 mV at ΔT = 500 K. The obtained maxima, I_{max} and P_{max}, for the module are 563.6 mA and 174.3 mW, respectively, at ΔT = 500 K. Although this performance is inadequate for practical use, there is much room for improvement in the quality of element, as mentioned above, such as the development of better electrode metals for Mg_2Si and optimization of the sintering process. Additionally, there is much room for improvement in the module architecture, as discussed below.

Figure 7 shows the open-circuit voltage of PFM/9, which is given by dividing V_{OC} by the number of elements used in the module, for temperature differences, ΔT, ranging from 100 K to 500 K. The values of single pin–fin structure elements, PFE-a and PFE-b, and the calculated one are also shown in this figure to illustrate the effect of module assembly on V_{OC}. The measured V_{OC} of the single pin–fin structures is about 85% of the calculated one, while that of the module is about 57% of the calculated one. Compared with the single pin–fin structure

Table III. Number of elements used for the TE module and resistances of the TE elements and module

Sample Name	Number of Pin–Fin Elements	Total Resistance of Elements at RT (mΩ)	Measured Resistance of Module at RT (mΩ)
PFM	9	275	320

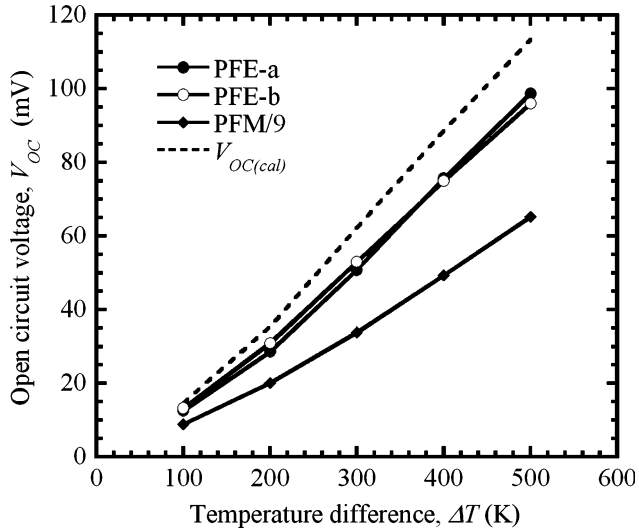

Fig. 7. Comparison of the open-circuit voltage between single pin–fin elements and the TE module.

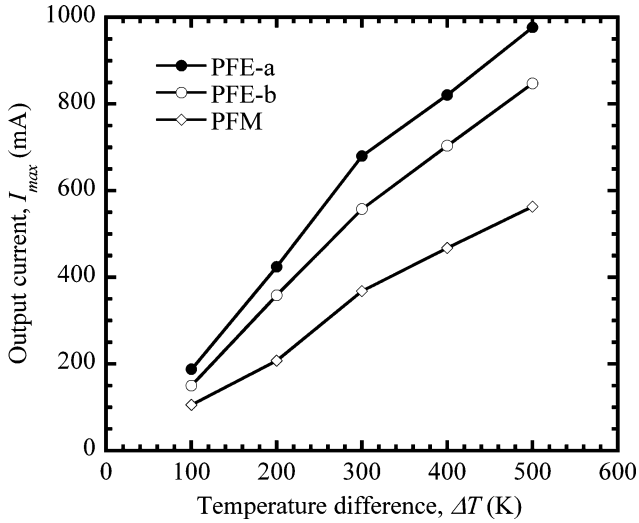

Fig. 8. Measured output current of samples PFE-a, PFE-b, and PFM as a function of temperature difference, ΔT, ranging from 100 K to 500 K.

elements, the V_{OC} of PFM/9 is considerably smaller. The reduced V_{OC} values of the modules may mainly be due to thermal conduction of the Ni terminals, because the thermal resistance of the Mg_2Si element and the Ni terminal are about 70 K/W to 136 K/W (at 373 K to 873 K) and about 150 K/W to 211 K/W (at 373 K to 873 K), respectively. This thermal conduction in the Ni terminals reduces the temperature difference between the hot and cold sides of the module, because the terminals are used to connect the hot side of one element with the cold side of its neighboring element. This is one of the important topics to consider when generating electric power from a uni-leg TE module. Another reason for the reduction in V_{OC} values of the module may be thermal radiation from the heat source to the cold side of the module via the large gaps between each element. In order to realize a high-performance TE module, the means of connecting each element of the uni-leg module must be further refined to prevent thermal radiation and conduction from the heat source.

The measured I_{max} of the module, PFM, is plotted against the temperature difference, ΔT, in Fig. 8, together with those of the single pin–fin structure elements, PFE-a and PFE-b. Compared with the single pin–fin elements, the values of I_{max} for the module are smaller. The average internal resistance of the elements in the module (30.6 mΩ) is lower than the internal resistance of the sample PFE-b (34 mΩ). Nevertheless, the I_{max} value of the module is lower than that of sample PFE-b. It would seem that the resistance of the Ni terminals and the contact resistance have resulted in a decrease in the output current of the module. Another reason for this is that the output voltage of each element used in the module is smaller than that of a single pin–fin element.

CONCLUSIONS

TE elements composed of n-type Mg_2Si were fabricated using a commercial polycrystalline Mg_2Si source. A new device architecture, the pin–fin structure, was used for the Mg_2Si TE elements in a uni-leg TE module, and the TE performance of both the elements and the module was evaluated. The observed values of the maximum output power of a single pin–fin element and the module were 50.9 mW and 174.3 mW, respectively, at ΔT = 500 K. From this investigation, it was found that the pin–fin structure is an effective architecture for a TE device. However the performance of our devices was greatly reduced due to electrical contact resistance. Therefore, improvement of the contact between the Mg_2Si and the electrode is needed in order to reduce contact resistance. With regard to module performance, it was found that there were large electrical and thermal losses. Therefore, it is necessary to investigate the module architecture thoroughly. However, this study also revealed that the uni-leg TE module using pin–fin structure elements can generate electricity at temperatures as high as 873 K. We confirmed that Mg_2Si and this structure are promising candidates for TE applications.

ACKNOWLEDGEMENTS

This work was partly supported by a Grant-in-Aid for Research (B) by the Japanese Ministry of Education, Science, Sports, and Culture.

REFERENCES

1. The 4th Assessment Report of the Intergovernmental Panel on Climate Change (IPCC), 2007.
2. T.M. Tritt and M.A. Subramanian, *MRS Bull.* 31, 188 (2006).

3. G.S. Nolas, J. Sharp, and H.J. Goldsmid, *Thermoelectrics* (Berlin: Springer, 2001), p. 146.
4. R.G. Morris, R.D. Redin, and G.C. Danielson, *Phys. Rev.* 109, 1909 (1958).
5. V.E. Borisenko, *Semiconducting Silicides* (Berlin: Springer, 2000), p. 285.
6. Y. Noda, H. Kon, Y. Furukawa, N. Otsuka, I.A. Nishida, and K. Masumoto, *Mater. Trans. JIM* 33, 845 (1992).
7. Y. Noda, H. Kon, Y. Furukawa, N. Otsuka, I.A. Nishida, and K. Masumoto, *Mater. Trans. JIM* 33, 851 (1992).
8. M. Fukano, T. Iida, K. Makino, M. Akasaka, Y. Oguni, and Y. Takanashi, *Crystal Growth of Mg_2Si by the Vertical Bridgman Method and the Doping Effect of Bi and Al on Thermoelectric Characteristics*, ed. T.P. Hogan, J. Yang, R. Funahashi, and T.M. Tritt (Mater. Res. Soc. Symp. Proc. 1044, 2008), pp. 247–252.
9. M.W. Heller and G.C. Danielson, *J. Phys. Chem. Solids* 23, 601 (1962).
10. S. Bose, H.N. Acharya, and H.D. Banerjee, *J. Mater. Sci.* 28, 5461 (1993).
11. M. Akasaka, T. Iida, T. Nemoto, J. Soga, J. Sato, K. Makino, M. Fukano, and Y. Takanashi, *J. Cryst. Growth* 304, 196 (2007).
12. M. Akasaka, T. Iida, A. Matsumoto, K. Yamanaka, Y. Takanashi, T. Imai, and N. Hamada, *J. Appl. Phys.* 104, 013703 (2008).
13. J. Tani and H. Kido, *Physica* B364, 218 (2005).
14. J. Tani and H. Kido, *J. Alloys Compd* 466, 335 (2008).
15. S. Lemonnier, C. Goupil, J. Noudem, and E. Guilmeau, *J. Appl. Phys.* 104, 014505 (2008).
16. Y. Oguni, T. Iida, A. Matsumoto, T. Nemoto, J. Onosaka1, H. Takaniwa, T. Sakamoto, D. Mori1, M. Akasaka, J. Sato, T. Nakajima, K. Nishio, and Y. Takanashi, *Formation of Transition-Metal-Based Ohmic Contacts to n-Mg_2Si by Plasma Activated Sintering*, ed. T.P. Hogan, J. Yang, R. Funahashi, and T.M. Tritt (Mater. Res. Soc. Symp. Proc. 1044, 2008), pp. 413–418.